

# Extending the FDTD GVADE method nonlinear polarization vector to include anisotropy

CALEB J. GRIMMS\* AND ROBERT D. NEVELS

*Department of Electrical and Computer Engineering, Texas A&M University, 188 Bizzel St, College Station, TX 77801, USA*

*\*cgrimms@tamu.org*

**Abstract:** In this paper the finite-difference time-domain general vector auxiliary differential equation method [Greene, J. H. and A. Taflove, *Opt. Express* **14**, 8305 (2006)], nonlinear polarization vector is extended to include anisotropy, in nonlinear isotropic media at optical frequencies. The theory is presented for extending the method in 3D Cartesian coordinates, and then simulation results are presented for the simplified 2D transverse magnetic polarization case, revisiting the fused silica example introduced in the 2006 paper including the anisotropic part of the nonlinear polarization vector. The simulation results including the anisotropic part of the polarization vector were compared with isotropic polarization vector simulation results.

## 1. Introduction

In this paper, the mathematics for the simulation of electromagnetic wave propagation in nonlinear isotropic material at optical frequencies using the general vector auxiliary differential equation finite-difference time-domain (GVADE FDTD) numerical method [1-3] are discussed, extending and generalizing the method's polarization vector to include an anisotropic part. The FDTD GVADE method models nonlinear behavior in nonlinear isotropic material using polarization current density from Ampere's law, which is related to the polarization vector by a time-derivative. The method assumes the nonlinear material is isotropic, meaning that without any electric or magnetic field applied the average material electromagnetic properties at a macroscopic level are the same in any direction, in contrast to many crystals for example where the material electromagnetic properties vary based on the direction. The FDTD GVADE method also assumes the polarization vectors in Maxwell's equations are isotropic, meaning "the polarization is assumed to line in the direction of the electric field" according to page 500 of [3] and the average material response, the electric flux density, is equally proportional to the applied electric field in any direction at a given point. However, electromagnetic wave propagation in some isotropic media can result in a polarization vector with an anisotropic part along with the isotropic part. This anisotropic part means the average material response, electric flux density, from an applied electric field is not the same in every direction or necessarily in the same direction as the applied field, requiring a tensor to describe properly. The purpose of this paper is to extend the FDTD GVADE method to simulate electromagnetic wave propagation in nonlinear isotropic material where both the isotropic part and the anisotropic part of the polarization vectors are present.

As a brief, non-comprehensive historical summary, optical frequency intensity dependent "self-induced" polarization changes have been observed since the 1960s [4-8], allowing phenomena like the "self-focusing" of electromagnetic waves to occur. During the 1960s and 1970s, the theory behind these phenomena began to be developed [9-15], and can be described and incorporated into Maxwell's equations using the nonlinear polarization vector. The classic review paper, discussing polarization vector at optical frequencies is R. W. Hellwarth's 1977 paper "Third-Order Optical Susceptibility of Liquids and Solids" [12]. Along with the general discussion of the polarization density vector in macroscopic material, Hellwarth's 1977 paper also presents a simplification for the polarization vector at optical frequencies in liquids and solids, the Born-Oppenheimer approximation, for isotropic media and anisotropic media like crystals with different types of symmetries such as cubic, hexagonal, trigonal, etc. In this paper

we are only considering isotropic media, and as such, will limit our discussion to the Born-Oppenheimer approximation of the polarization vector for isotropic media.

## 2. Theory

The advantage of FDTD based methods [16, 17] such as the FDTD GVADE method [1-3], is that they are generally considered to be more accurate than many other methods used in optics, such as the NLS equation. The potential increased accuracy is due to FDTD based methods needing fewer assumptions and simplifications than many other methods, solving the full vector Maxwell's equations directly, while requiring more computational resources as a result [18].

### 2.1 Maxwell's Equations in Isotropic Media Using Vector Notation

Beginning by writing Maxwell's equations for a nonmagnetic material without any free charges  $\rho$  or impressed current density vector  $\mathbf{J}$ :

$$\nabla \times \mathbf{H} = \frac{\partial \mathbf{D}}{\partial t}, \quad (1)$$

$$\nabla \times \mathbf{E} = -\mu_0 \frac{\partial \mathbf{H}}{\partial t}, \quad (2)$$

where  $\mathbf{H}$  is the instantaneous magnetic field vector and  $\mathbf{D}$  is the electric flux density. The Ampère-Maxwell law can be re-written in terms of the instantaneous electric field vector  $\mathbf{E}$ , polarization current density vector  $\mathbf{J}$  and polarization vector  $\mathbf{P}$ , where  $\mathbf{D} = \epsilon_0 \mathbf{E} + \mathbf{P}$  and  $\mathbf{J} = \frac{\partial \mathbf{P}}{\partial t}$ :

$$\nabla \times \mathbf{H} = \epsilon_0 \frac{\partial \mathbf{E}}{\partial t} + \mathbf{J}, \quad (3)$$

The polarization current density vector  $\mathbf{J}$  can be re-written by expanding the polarization vector  $\mathbf{P}$  into a series expansion of the electric field  $\mathbf{E}$ , where  $\mathbf{P} = \mathbf{P}^{(1)} + \mathbf{P}^{(2)} + \mathbf{P}^{(3)} + \dots$ . For many optical materials, the  $\mathbf{P}^{(2)}$  term is not present [12, 19]. The equations for  $\mathbf{P}^{(1)}$  and  $\mathbf{P}^{(3)}$  are

$$\mathbf{P}^{(1)}(\mathbf{r}, t) = \epsilon_0 \int_{-\infty}^{\infty} [\chi^{(1)}(t-t') \cdot \mathbf{E}(\mathbf{r}, t')] dt', \quad (4)$$

$$\mathbf{P}^{(3)}(\mathbf{r}, t) = \epsilon_0 \int_{-\infty}^{\infty} \int_{-\infty}^{\infty} \int_{-\infty}^{\infty} [\chi^{(3)}(t-t_1, t-t_2, t-t_3) : \mathbf{E}(\mathbf{r}, t_1) \mathbf{E}(\mathbf{r}, t_2) \mathbf{E}(\mathbf{r}, t_3)] dt_1 dt_2 dt_3, \quad (5)$$

where the tensor products of electric field with the susceptibility tensors  $\chi$  are shown [3, 19] using the “ $\cdot$ ” and “ $:$ ” notation. The “first-order” term  $\mathbf{P}^{(1)}$  is called “linear” due to  $\mathbf{P}^{(1)} \propto E$  while the “third order” term  $\mathbf{P}^{(3)}$  or  $\mathbf{P}^{\text{NL}}$  is called “nonlinear” due to  $\mathbf{P}^{(3)} \propto (E)^3$ . The linear  $\mathbf{P}^{(1)}$  term used here is the same as the FDTD GVADE method [1-3], modelling linear Lorentz dispersion using a Sellmeier expansion, and as a result, it will not be discussed here. The first-order susceptibility  $\chi^{(1)}$  is a rank 2 tensor containing 9 terms, and it is assumed to be isotropic here. The third-order susceptibility  $\chi^{(3)}$  is a rank 4 tensor containing 81 terms, which is also assumed to be isotropic, but it can lead to a polarization vector with an anisotropic part. For many materials at optical frequencies, the Born-Oppenheimer Approximation can be used to simplify  $\mathbf{P}^{(3)}$  [12], separating out the much faster “electronic” response from the slower “nuclear” response, assuming the “electronic” response is effectively instantaneous in comparison,

$$\mathbf{P}^{\text{NL}}(\mathbf{r}, t) = \mathbf{P}_{\text{cl}}^{\text{NL}}(\mathbf{r}, t) + \mathbf{P}_{\text{nu}}^{\text{NL}}(\mathbf{r}, t), \quad (6)$$

$$\mathbf{P}_{\text{cl}}^{\text{NL}}(\mathbf{r}, t) = \varepsilon_0 \chi_{\text{cl}}^{(3)} : [\mathbf{E}(\mathbf{r}, t) \mathbf{E}(\mathbf{r}, t) \mathbf{E}(\mathbf{r}, t)] = \varepsilon_0 \chi_{\text{cl}}^{(3)} \mathbf{E}(\mathbf{r}, t) |\mathbf{E}(\mathbf{r}, t)|^2, \quad (7)$$

$$\mathbf{P}_{\text{nu}}^{\text{NL}}(\mathbf{r}, t) = \varepsilon_0 \mathbf{E}(\mathbf{r}, t) \int_{-\infty}^{\infty} dt_1 [\chi_{\text{nu}}^{(3)}(t - t') : \mathbf{E}(\mathbf{r}, t') \mathbf{E}(\mathbf{r}, t')]. \quad (8)$$

For an isotropic media, this equation can be re-written as [10, 12, 19]

$$\mathbf{P}_{\text{nu}}^{\text{NL}} = \varepsilon_0 \mathbf{E}(\mathbf{r}, t) \int_{-\infty}^{\infty} [\chi_{\text{nu,a}}^{(3)}(t - t') |\mathbf{E}(\mathbf{r}, t')|^2] dt' + \varepsilon_0 \int_{-\infty}^{\infty} [ [\mathbf{E}(\mathbf{r}, t) \cdot \mathbf{E}(\mathbf{r}, t')] \chi_{\text{nu,b}}^{(3)}(t - t') \mathbf{E}(\mathbf{r}, t') ] dt'. \quad (9)$$

Hellwarth, Owyong and George in [10], called the first term of equation (9) containing  $\chi_{\text{nu,a}}^{(3)}$  the “isotropic” part of the nonlinear polarization vector due to each vector component of  $\mathbf{P}_{\text{nu}}^{\text{NL}}$  simply being  $E_x, E_y$  or  $E_z$  of  $\mathbf{E}(\mathbf{r}, t)$  multiplied by the same value,  $\varepsilon_0$  times the integral containing  $|\mathbf{E}(\mathbf{r}, t')|^2$  for a given  $(\mathbf{r}, t)$ , making it isotropic; while the second term of equation (9) containing  $\chi_{\text{nu,b}}^{(3)}$  was called the “anisotropic” part of the nonlinear polarization vector, due to each vector component of  $\mathbf{P}_{\text{nu}}^{\text{NL}}$ , not, simply being  $E_x, E_y$  or  $E_z$  of  $\mathbf{E}(\mathbf{r}, t)$  multiplied by the same value for a given  $(\mathbf{r}, t)$ . The “anisotropic” aspect can be seen more clearly in equations (33) to (40) and their discussion. This means that using the Born-Oppenheimer approximation in an isotropic media can have both isotropic and anisotropic nonlinear polarization vectors, which is not intuitive, and this will be further discussed in later sections.

## 2.2 FDTD GVADE Method Summary: Isotropic Media with an Isotropic Polarization Vector

The FDTD GVADE method [1-3] does require a few assumptions. First, the Born-Oppenheimer approximation is used with its corresponding assumptions. Second, the linear susceptibility  $\chi^{(1)}(\omega)$  is approximated using a Sellmeier pole expansion. This is used in the  $\mathbf{J}_{\text{Lorentz}}$  calculation, and it is also used to calculate the linear relative permittivity  $\varepsilon_r(\omega)$  and the linear refractive index  $n_0(\omega) = \sqrt{\varepsilon_r(\omega)}$  which are required for the  $\chi^{(3)}(t, \omega_c)$  calculation. Third, the electromagnetic wave is assumed to be operating at a center or carrier frequency,  $\omega_c$ , where the nonlinear susceptibility can be defined as  $\chi^{(3)}(t, \omega_c) = \chi_0^{(3)}(\omega_c) g(t)$ , allowing  $\chi_0^{(3)} = (4/3)c\varepsilon_0 [n_0(\omega_c)]^2 n_2$ , a constant calculated at  $\omega_c$ , to be pulled out of the nonlinear polarization vector integral [20, 21], where  $n_2$  is the third-order nonlinear refractive index and the normalized temporal response function  $g(t) = f_{\text{cl}} \delta_{\text{cl}}(t) + f_a g_a(t)$ . Fourth, the normalized nuclear temporal response function,  $g_a(t)$ , has a “closed form analytical” Fourier Transform, or can be approximated well by  $g_a(t) \approx \sum_m [f_m g_m(t)]$ , where  $g_m(t)$  have “closed form analytical” Fourier Transforms as described below.

The FDTD GVADE method [1-3] models electromagnetic wave propagation in nonlinear isotropic media at optical frequencies by accounting for the nonlinear behavior through the polarization current terms in Ampere’s law. The Ampere’s law equation is written at time-step  $n + 1/2$  approximating the time derivative of  $\mathbf{E}^{n+1/2}$  using a temporal finite-difference centered at  $n + 1/2$ , and is then solved for the electric fields at the time-step  $n + 1$  using the multi-dimensional Newton-Raphson method,

$$\nabla \times \mathbf{H}^{n+1/2} = \frac{\varepsilon_0}{\Delta t} (\mathbf{E}^{n+1} - \mathbf{E}^n) + \mathbf{J}_{\text{Lorentz}}^{n+1/2} + \mathbf{J}_{\text{cl}}^{n+1/2} + \mathbf{J}_{\text{nu,a}}^{n+1/2}, \quad (10)$$

where, the spatial derivatives in the  $\nabla \times \mathbf{H}^{n+1/2}$  term are approximated using spatial finite-differences of  $\mathbf{H}^{n+1/2}$  centered about the spatial location  $(x,y,z)$ . Then, using the electric fields at time-step  $n + 1$  as the new electric fields at time-step  $n$ , Faraday's law is solved for the magnetic fields using classic finite-difference time-domain update equations at the new time-step  $n + 1/2$ . This is repeated for each new time-step  $n$ .

The original FDTD GVADE method [1-3] solves the first convolution integral from equation (9), where  $\mathbf{J} = \frac{\partial \mathbf{P}}{\partial t}$ , as "auxiliary differential equations" (ADEs) which are solved as finite-difference update equations in Ampere's law using the Newton-Raphson method. As an example of the FDTD GVADE method process for solving a convolution integral using an auxiliary differential equation, the isotropic polarization vector term from equation (9) will be solved following the derivation from [2, 3], starting by defining the convolution integral as a scalar auxiliary variable,

$$S_{\text{nu},a}(t) = \int_{-\infty}^{\infty} \left[ \chi_{\text{nu},a}^{(3)}(t-t') |\mathbf{E}(\mathbf{r},t')|^2 \right] dt' = \chi_{\text{nu},a}^{(3)}(t) * |\mathbf{E}(t)|^2, \quad (11)$$

which will then be used to create an auxiliary differential equation. Choosing the  $g_{\text{nu},a}(t)$  from [3], which models the isotropic nonlinear behavior in silica using [2, 3, 22-24]

$$\chi_{\text{nu},a}^{(3)}(t) = f_a \chi_0^{(3)} g_{\text{nu},a}(t) = \chi_0^{(3)} \left( \frac{\tau_1^2 + \tau_2^2}{\tau_1 \tau_2^2} \right) e^{-t/\tau_2} \sin(t/\tau_1) U(t), \quad (12)$$

$$S_{\text{nu},a}(t) = \left[ \chi_0^{(3)} \left( \frac{\tau_1^2 + \tau_2^2}{\tau_1 \tau_2^2} \right) e^{-t/\tau_2} \sin(t/\tau_1) \right] * |\mathbf{E}(t)|^2. \quad (13)$$

The resulting auxiliary differential equation is found by taking the Fourier Transform of equation (13) and re-arranging and then taking the inverse Fourier Transform,

$$\omega_{\text{nu},a} \tilde{S}_{\text{nu},a}(t) + 2\delta_{\text{nu},a} \frac{\partial \tilde{S}_{\text{nu},a}(t)}{\partial t} + \frac{\partial^2 \tilde{S}_{\text{nu},a}(t)}{\partial t^2} = f_a \chi_0^{(3)} \omega_{\text{nu},a} |\mathbf{E}(t)|^2, \quad (14)$$

where  $\omega_{\text{nu},a} = \sqrt{(\tau_1^2 + \tau_2^2)/(\tau_1^2 \tau_2^2)}$  and  $\delta_{\text{nu},a} = 1/\tau_2$  [3]. This auxiliary differential equation is solved using a finite central difference equation centered around time-step  $n$ , where  $\frac{\partial S}{\partial t} \approx (S^{n+1} - S^{n-1})/(2\Delta t)$  and  $\frac{\partial^2 S}{\partial t^2} \approx (S^{n+1} - 2S^n + S^{n-1})/(\Delta t)^2$ . Then, the equation is re-arranged to solve for the scalar auxiliary variable at the new time-step  $n + 1$ ,

$$S_{\text{nu},a}^{n+1} = \left[ \frac{2 - \omega_{\text{nu},a}(\Delta t)^2}{\delta_{\text{nu},a}\Delta t + 1} \right] S_{\text{nu},a}^n + \left[ \frac{\delta_{\text{nu},a}\Delta t - 1}{\delta_{\text{nu},a}\Delta t + 1} \right] S_{\text{nu},a}^{n-1} + \left[ \frac{f_a \chi_0^{(3)} \omega_{\text{nu},a}^2 (\Delta t)^2}{\delta_{\text{nu},a}\Delta t + 1} \right] |\mathbf{E}^n(t)|^2. \quad (15)$$

The polarization current is then found by numerically differentiating  $\mathbf{J} = \frac{\partial \mathbf{P}}{\partial t}$  using a central difference centered around time-step  $n + 1/2$ ,

$$\mathbf{J}_{\text{nu},a}^{n+1/2} = \frac{\epsilon_0}{\Delta t} \left( |\mathbf{E}^{n+1}(t)|^2 S_{\text{nu},a}^{n+1}(t) - |\mathbf{E}^n(t)|^2 S_{\text{nu},a}^n(t) \right). \quad (16)$$

The FDTD GVADE method [1-3] solves for the linear and nonlinear electronic polarization currents as

$$\mathbf{J}_{\text{Lorentz}}^{n+1/2} = \frac{1}{2} \sum_{p=1}^3 \left[ (1 + \alpha_p) \mathbf{J}_{\text{Lorentz}_p}^n - \mathbf{J}_{\text{Lorentz}_p}^{n-1} + \frac{\gamma_p}{2\Delta t} (\mathbf{E}^{n+1} - \mathbf{E}^{n-1}) \right], \quad (17)$$

$$\mathbf{J}_{\text{el}}^{n+1/2} = \chi_0^{(3)} f_{\text{el}} \frac{\varepsilon_0}{\Delta t} \left\{ (|\mathbf{E}^{n+1}|)^2 \mathbf{E}^{n+1} - (|\mathbf{E}^n|)^2 \mathbf{E}^n \right\}. \quad (18)$$

Please see [3] for the full derivation. The FDTD GVADE method [1-3] uses only the isotropic nuclear polarization vector integral in its formulation represented by  $\mathbf{J}_{\text{nu,a}}^{n+1/2}$ . The purpose of this paper is to extend the method to include the anisotropic part of the polarization vector integral into the method using  $\mathbf{J}_{\text{nu,b}}^{n+1/2}$ .

### 2.3 The Polarization Vector and Rank 4 Susceptibility Tensor Using Index Notation

To properly understand the rank 4 susceptibility tensor composed of 81 terms, the third order polarization vector equations from the prior section, and to understand the following sections, index notation is introduced. The summations are explicitly shown in the following equations for clarity. Re-writing equation (5) using index notation ( $i = x, y, x$ ) [12],

$$P_i^{\text{NL}}(\mathbf{r}, t) = \varepsilon_0 \sum_j \sum_k \sum_l \int_{-\infty}^{\infty} \int_{-\infty}^{\infty} \int_{-\infty}^{\infty} \left[ \chi_{ijkl}^{(3)}(t - t_1, t - t_2, t - t_3) E_j(\mathbf{r}, t_1) E_k(\mathbf{r}, t_2) E_l(\mathbf{r}, t_3) \right] dt_1 dt_2 dt_3. \quad (19)$$

Next, re-writing equations (7) and (8) following [12], where  $P_i^{\text{NL}}(\mathbf{r}, t) = P_{\text{el},i}^{\text{NL}}(\mathbf{r}, t) + P_{\text{nu},i}^{\text{NL}}(\mathbf{r}, t)$ ,

$$P_{\text{el},i}^{\text{NL}}(\mathbf{r}, t) = \varepsilon_0 \sum_j \sum_k \sum_l \chi_{\text{el},ijkl}^{(3)} E_j(\mathbf{r}, t) E_k(\mathbf{r}, t) E_l(\mathbf{r}, t), \quad (20)$$

$$P_{\text{nu},i}^{\text{NL}}(\mathbf{r}, t) = \varepsilon_0 \sum_j \sum_k \sum_l E_j(\mathbf{r}, t) \int_{-\infty}^{\infty} \left[ \chi_{\text{nu},ijkl}^{(3)}(t - t') E_k(\mathbf{r}, t') E_l(\mathbf{r}, t') \right] dt'. \quad (21)$$

The general rank 4 isotropic susceptibility tensor used for isotropic media is shown for the “nuclear” part [12, 25, 26], where  $\delta_{ij}=1$  when  $i = j$  and  $\delta_{ij}=0$  when  $i \neq j$ :

$$\chi_{\text{nu},ijkl}^{(3)}(t) = \chi_{\text{nu,a}}^{(3)}(t) \delta_{ij} \delta_{kl} + \frac{1}{2} \chi_{\text{nu,b}}^{(3)}(t) (\delta_{ik} \delta_{jl} + \delta_{il} \delta_{jk}). \quad (22)$$

The term  $\chi_{\text{nu,a}}^{(3)}(t) (\delta_{ij} \delta_{kl})$ , after being plugged into equation (21), produces the isotropic part of the nonlinear polarization vector,

$$P_{\text{nu,a},i}^{\text{NL}}(\mathbf{r}, t) = \varepsilon_0 \sum_j \sum_k \sum_l E_j(\mathbf{r}, t) \int_{-\infty}^{\infty} \left[ \chi_{\text{nu,a}}^{(3)}(t - t') \delta_{ij} \delta_{kl} E_k(\mathbf{r}, t') E_l(\mathbf{r}, t') \right] dt', \quad (23)$$

and the  $(1/2) \chi_{\text{nu,b}}^{(3)}(t) (\delta_{ik} \delta_{jl} + \delta_{il} \delta_{jk})$  term, after being plugged into equation (21), produces the anisotropic part of the nonlinear polarization vector,

$$P_{\text{nu,b},i}^{\text{NL}}(\mathbf{r}, t) = \varepsilon_0 \sum_j \sum_k \sum_l E_j(\mathbf{r}, t) \int_{-\infty}^{\infty} \left[ \frac{1}{2} \chi_{\text{nu,b}}^{(3)}(t - t') (\delta_{ik} \delta_{jl} + \delta_{il} \delta_{jk}) E_k(\mathbf{r}, t') E_l(\mathbf{r}, t') \right] dt'. \quad (24)$$

The electronic contribution, being much faster than the nuclear response, is [27] approximated as being instantaneous using  $g_{\text{el}}(t) = \delta(t)$  [12]:

$$\chi_{\text{el},ijkl}^{(3)}(t) = \chi_{\text{el}}^{(3)} \delta(t) \frac{1}{3} (\delta_{ij} \delta_{kl} + \delta_{ik} \delta_{jl} + \delta_{il} \delta_{jk}). \quad (25)$$

When equation (22) is plugged into equation (21) it results in equation (9), and when equation (25) is plugged into equation (20) it results in equation (8). The electronic contribution and the nuclear contributions can also be written together as,

$$\chi_{ijkl}^{(3)}(t) = \frac{1}{3}\chi_{el}^{(3)}\delta(t)(\delta_{ij}\delta_{kl}+\delta_{ik}\delta_{jl}+\delta_{il}\delta_{jk}) + \chi_{nu,a}^{(3)}(t)\delta_{ij}\delta_{kl} + \frac{1}{2}\chi_{nu,b}^{(3)}(t)(\delta_{ik}\delta_{jl}+\delta_{il}\delta_{jk}), \quad (26)$$

where  $\chi^{(3)}(t)$  from equation (5) is related to the index notation  $\chi_{ijkl}^{(3)}(t)$  using the summation of the unit vector dyadic products, dyads,  $\hat{\mathbf{a}}_i\hat{\mathbf{a}}_j$  and  $\hat{\mathbf{a}}_k\hat{\mathbf{a}}_l$  with  $\chi_{ijkl}^{(3)}(t)$ ,

$$\chi^{(3)}(t) = \sum_i \sum_j \sum_k \sum_l \hat{\mathbf{a}}_i\hat{\mathbf{a}}_j \chi_{ijkl}^{(3)}(t) \hat{\mathbf{a}}_k\hat{\mathbf{a}}_l. \quad (27)$$

A constant scalar value  $\chi_0^{(3)}$  can be pulled out of  $\chi_{ijkl}^{(3)}(t)$ , leading to,

$$\chi_{ijkl}^{(3)}(t) = \chi_0^{(3)} g_{ijkl}(t) = \chi_0^{(3)} \left[ \frac{1-f_R}{3} \delta(t)(\delta_{ij}\delta_{kl} + \delta_{ik}\delta_{jl} + \delta_{il}\delta_{jk}) + f_a g_a(t)\delta_{ij}\delta_{kl} + \frac{1}{2}f_b g_b(t)(\delta_{ik}\delta_{jl} + \delta_{il}\delta_{jk}) \right], \quad (28)$$

where  $g_a(t)$  and  $g_b(t)$  are the normalized isotropic and anisotropic parts of the normalized nuclear response function  $g_{ijkl}(t)$  according to [28], normalized so that  $\int_0^\infty g_a(t)dt=1$  and  $\int_0^\infty g_b(t)dt=1$ , with relative strengths  $f_a$  and  $f_b$  defined as  $f_R=f_a+f_b$  and  $f_{el}=(1-f_R)$ . The normalization of  $g_{ijkl}(t)$  can be seen by looking at  $i=j=k=l=x$ , resulting in  $g_{xxxx}(t) = [(1-f_R)\delta(t) + f_a g_a(t) + f_b g_b(t)]\delta_{xx}\delta_{xx}$ , where  $\int_0^\infty g_{xxxx}(t)dt=1$ , since  $\delta_{xx}\delta_{xx} = 1$  [29]. This example shows that the 1/3 and the 1/2 factors in equation (28), are necessary for normalization due to the tensor nature of the polarization vector. For example, the summation of the electronic  $(\delta_{ij}\delta_{kl} + \delta_{ik}\delta_{jl} + \delta_{il}\delta_{jk})$  term results in  $3(\epsilon_0\chi_{el}^{(3)}\mathbf{E}(\mathbf{r},t)|\mathbf{E}(\mathbf{r},t)|^2)$  requiring the 1/3 factor to normalize the term. In a similar manner the summation of the nuclear ‘‘anisotropic’’  $(\delta_{ik}\delta_{jl} + \delta_{il}\delta_{jk})$  term results in two times the anisotropic convolution integral, requiring the 1/2 factor to normalize it. This definition of  $\chi_{ijkl}^{(3)}(t)$  can be plugged into,

$$P_i^{NL}(\mathbf{r},t) = \epsilon_0 \sum_j \sum_k \sum_l E_j(\mathbf{r},t) \int_{-\infty}^{\infty} [\chi_{ijkl}^{(3)}(t-t')E_k(\mathbf{r},t')E_l(\mathbf{r},t')] dt', \quad (29)$$

resulting in equations (6), (7) and (8). This substitution allows equations (20), (23) and (24) to be re-written in terms of  $f_{el}$ ,  $f_a$  and  $f_b$  as,

$$P_{el,i}^{NL}(\mathbf{r},t) = \epsilon_0\chi_0^{(3)} \sum_j \sum_k \sum_l \frac{1}{3}f_{el}\delta(t)(\delta_{ij}\delta_{kl} + \delta_{ik}\delta_{jl} + \delta_{il}\delta_{jk}) E_j(\mathbf{r},t)E_k(\mathbf{r},t)E_l(\mathbf{r},t), \quad (30)$$

$$P_{nu,a,i}^{NL}(\mathbf{r},t) = \epsilon_0\chi_0^{(3)} \sum_j \sum_k \sum_l E_j(\mathbf{r},t) \int_{-\infty}^{\infty} [f_a g_a(t-t')\delta_{ij}\delta_{kl} E_k(\mathbf{r},t')E_l(\mathbf{r},t')] dt', \quad (31)$$

$$P_{nu,b,i}^{NL}(\mathbf{r},t) = \epsilon_0\chi_0^{(3)} \sum_j \sum_k \sum_l E_j(\mathbf{r},t) \int_{-\infty}^{\infty} \left[ \frac{1}{2}f_b g_b(t-t')(\delta_{ik}\delta_{jl}+\delta_{il}\delta_{jk}) E_k(\mathbf{r},t')E_l(\mathbf{r},t') \right] dt', \quad (32)$$

which are equivalent to equations (7) and (9).

## 2.4 Extended FDTD GVADE Method: Including the Anisotropic Part of the Polarization Vector

The result of including the anisotropic part of the polarization vector is more required convolution integrals and more auxiliary differential equations. Writing out the vector components of the anisotropic part of the nuclear polarization vector, from either equation (24) or the anisotropic integral from equation (9), in terms of scalar auxiliary variables,  $S_{b,kl}(t)$ :

$$P_{\text{nu},b,x}^{(3)}(t) = \varepsilon_0 [E_x(t)S_{b,xx}(t) + E_y(t)S_{b,xy}(t) + E_z(t)S_{b,xz}(t)], \quad (33)$$

$$P_{\text{nu},b,y}^{(3)}(t) = \varepsilon_0 [E_x(t)S_{b,xy}(t) + E_y(t)S_{b,yy}(t) + E_z(t)S_{b,yz}(t)], \quad (34)$$

$$P_{\text{nu},b,z}^{(3)}(t) = \varepsilon_0 [E_x(t)S_{b,xz}(t) + E_y(t)S_{b,yz}(t) + E_z(t)S_{b,zz}(t)], \quad (35)$$

where,

$$S_{b,kl}(t) = \int_{-\infty}^{\infty} [\chi_0^{(3)} f_b g_b(t-t') E_k(t') E_l(t)] dt' = f_b \chi_0^{(3)} (g_b(t) * [E_k(t) E_l(t)]). \quad (36)$$

For comparison, the isotropic nuclear polarization vector components are

$$P_{\text{nu},a,x}^{(3)}(t) = \varepsilon_0 E_x(t) [S_{a,xx}(t) + S_{a,yy}(t) + S_{a,zz}(t)] = E_x(t) S_a(t), \quad (37)$$

$$P_{\text{nu},a,y}^{(3)}(t) = \varepsilon_0 E_y(t) [S_{a,xx}(t) + S_{a,yy}(t) + S_{a,zz}(t)] = E_y(t) S_a(t), \quad (38)$$

$$P_{\text{nu},a,z}^{(3)}(t) = \varepsilon_0 E_z(t) [S_{a,xx}(t) + S_{a,yy}(t) + S_{a,zz}(t)] = E_z(t) S_a(t). \quad (39)$$

It can be seen that the “isotropic” part of the polarization vector is defined as isotropic since the electric fields in each Cartesian direction,  $E_x$ ,  $E_y$ , and  $E_z$  are all multiplied by the same term,  $S_a(t)$ , as described by  $P_{\text{nu},a,i}^{(3)}(t) = \varepsilon_0 E_i(t) S_a(t)$  or equivalently  $\mathbf{P}_{\text{nu},a}^{(3)}(t) = \varepsilon_0 \mathbf{E}(t) S_a(t)$ . The “anisotropic” term is called anisotropic because  $P_{\text{nu},b,i}^{(3)}(t) \neq E_i(t) S_b(t)$ , but rather a rank 2 tensor  $\mathbf{S}_b$  multiplied by  $\varepsilon_0$ , relates  $\mathbf{P}_{\text{nu},b}^{(3)}(t)$  and  $\mathbf{E}(t)$ ,

$$\mathbf{P}_{\text{nu},b}^{(3)}(t) = \varepsilon_0 \mathbf{S}_b \mathbf{E}(t) = \varepsilon_0 \begin{bmatrix} S_{b,xx}(t) & S_{b,xy}(t) & S_{b,xz}(t) \\ S_{b,xy}(t) & S_{b,yy}(t) & S_{b,yz}(t) \\ S_{b,xz}(t) & S_{b,yz}(t) & S_{b,zz}(t) \end{bmatrix} \begin{bmatrix} E_x(t) \\ E_y(t) \\ E_z(t) \end{bmatrix}. \quad (40)$$

The anisotropic part of the polarization vector can be seen to require nine extra convolution integrals,  $S_{b,kl}(t)$ , for the full 3D case, in addition to the one convolution integral,  $S_a(t)$ , required for the isotropic part of the polarization vector.

## 2.5 Anisotropic Polarization Vector Convolution Integrals and Auxiliary Differential Equations for Silica Anisotropic Temporal Response Function

For the anisotropic part of the polarization vector, a similar process to Section 2.2 is used to create and solve the auxiliary differential equations corresponding to equations (33)-(36). As an example, the normalized function  $g_b(t)$  which represents the anisotropic response of silica is [19, 29]

$$g_b(t) = \left( \frac{2\tau_b - t}{\tau_b^2} \right) e^{-t/\tau_b} U(t) = C_b (2\tau_b - t) e^{-t/\tau_b} U(t), \quad (41)$$

where  $C_b = 1/\tau_b^2$ .

The scalar auxiliary variable is split into two components  $S_{b,kl}(t) = S_{b1,kl}(t) + S_{b2,kl}(t)$ , so that known closed form Fourier Transforms exist,

$$S_{b1,kl}(t) = f_b \chi_0^{(3)} \left( g_{b,1}(t) * [E_k(t)E_l(t)] \right), \quad (42)$$

$$S_{b2,kl}(t) = f_b \chi_0^{(3)} \left( g_{b,2}(t) * [E_k(t)E_l(t)] \right), \quad (43)$$

where  $g_{b,1}(t) = C_b(2\tau_b)e^{-t/\tau_b} U(t)$  and  $g_{b,2}(t) = -C_b t e^{-t/\tau_b} U(t)$ . Taking the Fourier Transform of equation (42), with  $\omega_b = 1/\tau_b$ ,

$$\tilde{S}_{b1,kl}(\omega) = f_b \chi_0^{(3)} \left( \tilde{g}_{b,1}(\omega) \cdot \mathcal{F}[E_k(t)E_l(t)] \right), \quad (44)$$

with,

$$\tilde{g}_{b,1}(\omega) = C_b \left( \frac{2\tau_b}{\omega_b + j\omega} \right). \quad (45)$$

Equation (45) is plugged into (44), multiplied on both sides by  $(\omega_b + j\omega)$  and re-arranged,

$$(\omega_b + j\omega)\tilde{S}_{b1,kl}(\omega) = f_b \chi_0^{(3)} C_b 2\tau_b \cdot \mathcal{F}[E_k(t)E_l(t)]. \quad (46)$$

The inverse Fourier transform is taken, resulting in the  $S_{b1,kl}$  auxiliary differential equation,

$$\omega_b S_{b1,kl}(t) + \frac{\partial S_{b1,kl}(t)}{\partial t} = f_b \chi_0^{(3)} C_b 2\tau_b [E_k(t)E_l(t)]. \quad (47)$$

Next, taking the Fourier Transform of equation (43), with again  $\omega_b = 1/\tau_b$ ,

$$\tilde{S}_{b2,kl}(\omega) = f_b \chi_0^{(3)} \left( \tilde{g}_{b,2}(\omega) \cdot \mathcal{F}[E_k(t)E_l(t)] \right), \quad (48)$$

with,

$$\tilde{g}_{b,2}(\omega) = -C_b \left( \frac{1}{(\omega_b + j\omega)^2} \right). \quad (49)$$

Equation (49) is plugged into (48), multiplied on both sides by  $(\omega_b + j\omega)^2$  and re-arranged,

$$[\omega_b^2 + 2\omega_b(j\omega) + (j\omega)^2] \tilde{S}_{b2,kl}(\omega) = -f_b \chi_0^{(3)} C_b \cdot \mathcal{F}[E_k(t)E_l(t)]. \quad (50)$$

The inverse Fourier transform is taken, resulting in the  $S_{b2,kl}$  auxiliary differential equation,

$$\omega_b^2 S_{b2,kl}(t) + 2\omega_b \frac{\partial S_{b2,kl}(t)}{\partial t} + \frac{\partial^2 S_{b2,kl}(t)}{\partial t^2} = -f_b \chi_0^{(3)} C_b [E_k(t)E_l(t)]. \quad (51)$$

Explicit time-stepping relations are created for equations (47) and (51) using central difference approximations in time about time-step  $n$ , where  $\frac{\partial S}{\partial t} \approx (S^{n+1} - S^{n-1})/(2\Delta t)$  and  $\frac{\partial^2 S}{\partial t^2} \approx (S^{n+1} - 2S^n + S^{n-1})/(\Delta t)^2$ , and then each equation is solved for  $S^{n+1}$ :

$$S_{b1,kl}^{n+1} = [-2\omega_b(\Delta t)] S_{b1,kl}^n + S_{b1,kl}^{n-1} + [4(\Delta t) f_b \chi_0^{(3)} C_b \tau_b] E_k^n(t) E_l^n(t), \quad (52)$$

$$S_{b2,kl}^{n+1} = \left[ \frac{2 - \omega_b^2 (\Delta t)^2}{\omega_b \Delta t + 1} \right] S_{b2,kl}^n + \left[ \frac{\omega_b \Delta t - 1}{\omega_b \Delta t + 1} \right] S_{b2,kl}^{n-1} + \left[ -\frac{(\Delta t)^2 f_b \chi_0^{(3)} C_b}{(\omega_b \Delta t + 1)} \right] E_k^n(t) E_l^n(t). \quad (53)$$

Lastly,  $\mathbf{J}_{\text{nu},b}(t) = \frac{\partial}{\partial t} \mathbf{P}_{\text{nu},b}$  is numerically differentiated by central differencing equations (33) to (35), centered around time-step  $n + 1/2$  to get the polarization current,

$$\begin{aligned} J_{k,\text{nu},b}^{n+1/2} = & \frac{\varepsilon_0}{\Delta t} [E_x^{n+1}(t) S_{b,kx}^{n+1}(t) - E_x^n(t) S_{b,kx}^n(t)] + \frac{\varepsilon_0}{\Delta t} [E_y^{n+1}(t) S_{b,ky}^{n+1}(t) \\ & - E_y^n(t) S_{b,ky}^n(t)] + \frac{\varepsilon_0}{\Delta t} [E_z^{n+1}(t) S_{b,kz}^{n+1}(t) - E_z^n(t) S_{b,kz}^n(t)]. \end{aligned} \quad (54)$$



## 2.6 Solving Ampere's Law for the Electric Fields Using the Newton Raphson Method

Following and extending the approach from [1-3], the electric field at time-step  $n + 1$  is determined using the Newton-Raphson method to solve Ampere's law at time-step  $n + 1/2$ ,

$$\nabla \times \mathbf{H}^{n+1/2} = \frac{\epsilon_0}{\Delta t} (\mathbf{E}^{n+1} - \mathbf{E}^n) + \mathbf{J}_{\text{Lorentz}}^{n+1/2} + \mathbf{J}_{\text{el}}^{n+1/2} + \mathbf{J}_{\text{nu,a}}^{n+1/2} + \mathbf{J}_{\text{nu,b}}^{n+1/2}. \quad (55)$$

Plugging in the polarization current expressions into Ampere's law at time step  $n + 1/2$ , results in an equation which can be used as part of the Newton-Raphson method to determine  $\mathbf{E}^{n+1}$ ,

$$\begin{aligned} \begin{bmatrix} X \\ Y \\ Z \end{bmatrix} &= -\nabla \times \mathbf{H}^{n+1/2} + \frac{\epsilon_0}{\Delta t} (\mathbf{E}^{n+1} \\ &- \mathbf{E}^n) + \frac{1}{2} \sum_{p=1}^3 \left[ (1 + \alpha_p) \mathbf{J}_{\text{Lorentz}p}^n \right. \\ &- \left. \mathbf{J}_{\text{Lorentz}p}^{n-1} + \frac{\gamma_p}{2\Delta t} (\mathbf{E}^{n+1} - \mathbf{E}^{n-1}) \right] + \chi_0^{(3)} f_{\text{el}} \frac{\epsilon_0}{\Delta t} \{ (|\mathbf{E}^{n+1}|)^2 \mathbf{E}^{n+1} \\ &- (|\mathbf{E}^n|^2 \mathbf{E}^n) \} + \frac{\epsilon_0}{\Delta t} (\mathbf{E}^{n+1} S_a^{n+1} - \mathbf{E}^n S_a^n) + \frac{\epsilon_0}{\Delta t} (\mathbf{S}_b^{n+1} \mathbf{E}^{n+1} \\ &- \mathbf{S}_b^n \mathbf{E}^n). \end{aligned} \quad (56)$$

The Newton-Raphson method solves for the electric field by iterative guessing based on the Jacobian Matrix, until  $X$ ,  $Y$  and  $Z$  become sufficiently close zero, using [30]

$$\begin{bmatrix} E_x^{n+1} \\ E_y^{n+1} \\ E_z^{n+1} \end{bmatrix}_{g+1} = \begin{bmatrix} E_x^{n+1} \\ E_y^{n+1} \\ E_z^{n+1} \end{bmatrix}_g - \left( \mathbf{M}^{-1} \begin{bmatrix} X \\ Y \\ Z \end{bmatrix} \right) \Big|_g. \quad (57)$$

Each Newton-Raphson iteration guess values of  $E_x^{n+1}$ ,  $E_y^{n+1}$  and  $E_z^{n+1}$  at guess number "g", are used to then estimate the next iteration values of  $E_x^{n+1}$ ,  $E_y^{n+1}$  and  $E_z^{n+1}$  at guess number "g+1". The Jacobian matrix  $\mathbf{M}$  is defined by  $\partial(X, Y, Z)/\partial(E_x^{n+1}, E_y^{n+1}, E_z^{n+1})$ ,

$$M_{11} = \frac{1}{4\Delta t} \sum_{p=1}^3 \gamma_p + \frac{\epsilon_0}{\Delta t} \left[ 1 + f_{\text{el}} \chi_0^{(3)} \{ 3(E_x^{n+1})^2 + (E_y^{n+1})^2 + (E_z^{n+1})^2 \} + S_a^{n+1} + S_{b,xx}^{n+1} \right], \quad (58)$$

$$M_{22} = \frac{1}{4\Delta t} \sum_{p=1}^3 \gamma_p + \frac{\epsilon_0}{\Delta t} \left[ 1 + f_{\text{el}} \chi_0^{(3)} \{ (E_x^{n+1})^2 + 3(E_y^{n+1})^2 + (E_z^{n+1})^2 \} + S_a^{n+1} + S_{b,yy}^{n+1} \right], \quad (59)$$

$$M_{33} = \frac{1}{4\Delta t} \sum_{p=1}^3 \gamma_p + \frac{\epsilon_0}{\Delta t} \left[ 1 + f_{\text{el}} \chi_0^{(3)} \{ (E_x^{n+1})^2 + (E_y^{n+1})^2 + 3(E_z^{n+1})^2 \} + S_a^{n+1} + S_{b,zz}^{n+1} \right], \quad (60)$$

$$M_{12} = M_{21} = f_{\text{el}} \frac{\epsilon_0 \chi_0^{(3)}}{\Delta t} 2E_x^{n+1} E_y^{n+1} + \frac{\epsilon_0}{\Delta t} (S_{b,xy}^{n+1}), \quad (61)$$

$$M_{13} = M_{31} = f_{\text{el}} \frac{\epsilon_0 \chi_0^{(3)}}{\Delta t} 2E_x^{n+1} E_z^{n+1} + \frac{\epsilon_0}{\Delta t} (S_{b,xz}^{n+1}), \quad (62)$$

$$M_{23} = M_{32} = f_{\text{el}} \frac{\epsilon_0 \chi_0^{(3)}}{\Delta t} 2E_y^{n+1} E_z^{n+1} + \frac{\epsilon_0}{\Delta t} (S_{b,yz}^{n+1}). \quad (63)$$

Note the off-diagonal terms of the Jacobian now have an extra term corresponding to,  $S_{b,xy}^{n+1}$ ,  $S_{b,xz}^{n+1}$ ,  $S_{b,yz}^{n+1}$ , that was not present in the isotropic polarization vector FDTD GVADE method, along with the diagonal terms adding  $S_{b,xx}^{n+1}$ ,  $S_{b,yy}^{n+1}$ ,  $S_{b,zz}^{n+1}$ .

## 2.7 Special Case: 2D Transverse Magnetic to z

An important special case, transverse magnetic to z, is simpler than examples requiring the full 3D Maxwell's equations. However, it does still include a few components of the anisotropic polarization vector, allowing for an anisotropic case to be simulated while requiring less computational resources. In the case where the field components do not depend on the y coordinate, this causes the  $\frac{\partial}{\partial y}$  terms from Maxwell's equations to be zero, leaving only the  $H_y$ ,  $E_x$  and  $E_z$  fields,

$$(\nabla \times \mathbf{E})_{y,2D} = \frac{\partial E_x}{\partial z} - \frac{\partial E_z}{\partial x} = -\mu_0 \frac{\partial H_y}{\partial t}, \quad (64)$$

$$(\nabla \times \mathbf{H})_{x,2D} = -\frac{\partial H_y}{\partial z} = \varepsilon_0 \frac{\partial E_x}{\partial t} + J_x, \quad (65)$$

$$(\nabla \times \mathbf{H})_{z,2D} = \frac{\partial H_y}{\partial x} = \varepsilon_0 \frac{\partial E_z}{\partial t} + J_z. \quad (66)$$

The nonlinear polarization vector  $\mathbf{P}^{(3)}(t)$  simplifies, but it still includes anisotropic terms,

$$P_x^{\text{NL}}(t) = \varepsilon_0 [\chi_{\text{el}}^{(3)} E_x(t) |\mathbf{E}(t)|^2 + E_x(t) S_a(t) + E_x(t) S_{b,xx}(t) + E_z(t) S_{b,xz}(t)], \quad (67)$$

$$P_z^{\text{NL}}(t) = \varepsilon_0 [\chi_{\text{el}}^{(3)} E_z(t) |\mathbf{E}(t)|^2 + E_z(t) S_a(t) + E_x(t) S_{b,xz}(t) + E_z(t) S_{b,zz}(t)]. \quad (68)$$

The Newton-Raphson method simplifies to  $\mathbf{E}^{n+1} = \hat{\mathbf{a}}_x E_x^{n+1} + \hat{\mathbf{a}}_z E_z^{n+1}$ ,

$$\begin{aligned} \begin{bmatrix} X \\ Z \end{bmatrix} &= -\nabla \times \mathbf{H}^{n+1/2} + \frac{\varepsilon_0}{\Delta t} (\mathbf{E}^{n+1} \\ &\quad - \mathbf{E}^n) + \frac{1}{2} \sum_{p=1}^3 \left[ (1 + \alpha_p) \mathbf{J}_{\text{Lorentz}p}^n \right. \\ &\quad \left. - \mathbf{J}_{\text{Lorentz}p}^{n-1} + \frac{\gamma_p}{2\Delta t} (\mathbf{E}^{n+1} - \mathbf{E}^{n-1}) \right] + \chi_0^{(3)} f_{\text{el}} \frac{\varepsilon_0}{\Delta t} \left\{ (|\mathbf{E}^{n+1}|)^2 \mathbf{E}^{n+1} \right. \\ &\quad \left. - (|\mathbf{E}^n|)^2 \mathbf{E}^n \right\} + \frac{\varepsilon_0}{\Delta t} (\mathbf{E}^{n+1} S_a^{n+1} - \mathbf{E}^n S_a^n) \\ &\quad + \left[ \frac{\varepsilon_0}{\Delta t} (E_x^{n+1} S_{b,xx}^{n+1} - E_x^n S_{b,xx}^n) + \frac{\varepsilon_0}{\Delta t} (E_z^{n+1} S_{b,xz}^{n+1} - E_z^n S_{b,xz}^n) \right] \\ &\quad \left. + \left[ \frac{\varepsilon_0}{\Delta t} (E_x^{n+1} S_{b,xz}^{n+1} - E_x^n S_{b,xz}^n) + \frac{\varepsilon_0}{\Delta t} (E_z^{n+1} S_{b,zz}^{n+1} - E_z^n S_{b,zz}^n) \right] \right\}, \end{aligned} \quad (69)$$

where,

$$\begin{bmatrix} E_x^{n+1} \\ E_z^{n+1} \end{bmatrix}_{g+1} = \begin{bmatrix} E_x^{n+1} \\ E_z^{n+1} \end{bmatrix}_g - (\mathbf{M}_{\text{TM}}^{-1} \begin{bmatrix} X \\ Z \end{bmatrix}) \Big|_g, \quad (70)$$

$$M_{\text{TM},11} = \frac{1}{4\Delta t} \sum_{p=1}^3 \gamma_p + \frac{\varepsilon_0}{\Delta t} \left[ I + f_{\text{el}} \chi_0^{(3)} \left\{ 3(E_x^{n+1})^2 + (E_z^{n+1})^2 \right\} + S_a^{n+1} + S_{b,xx}^{n+1} \right], \quad (71)$$

$$M_{\text{TM},22} = \frac{1}{4\Delta t} \sum_{p=1}^3 \gamma_p + \frac{\varepsilon_0}{\Delta t} \left[ I + f_{\text{el}} \chi_0^{(3)} \left\{ (E_x^{n+1})^2 + 3(E_z^{n+1})^2 \right\} + S_a^{n+1} + S_{b,zz}^{n+1} \right], \quad (72)$$

$$M_{\text{TM},12} = M_{\text{TM},21} = f_{\text{el}} \frac{\varepsilon_0 \chi_0^{(3)}}{\Delta t} 2E_x^{n+1} E_z^{n+1} + \frac{\varepsilon_0}{\Delta t} (S_{b,xz}^{n+1}). \quad (73)$$

Note the off-diagonal terms of the Jacobian now have an extra term corresponding to,  $S_{b,xz}^{n+1}$ , that was not present in the isotropic polarization vector FDTD GVADE method.

## 2.8 Special Case: Transverse Electric to z

Another important special case is the transverse electric to z. This case is simpler than the full 3D Maxwell's equations, removing all anisotropic components of the polarization vector due to only having one electric field component, matching the isotropic polarization vector FDTD GVADE method. In the case where the field components do not depend on the y coordinate, the  $\frac{\partial}{\partial y}$  terms from Maxwell's equations become zero, leaving only the  $E_y$ ,  $H_x$  and  $H_z$  fields,

$$(\nabla \times \mathbf{H})_{y,2D} = \frac{\partial H_x}{\partial z} - \frac{\partial H_z}{\partial x} = \varepsilon_0 \frac{\partial E_y}{\partial t} + J_y, \quad (74)$$

$$(\nabla \times \mathbf{E})_{x,2D} = \frac{\partial E_y}{\partial z} = \mu_0 \frac{\partial H_x}{\partial t}, \quad (75)$$

$$(\nabla \times \mathbf{E})_{z,2D} = \frac{\partial E_y}{\partial x} = -\mu_0 \frac{\partial H_z}{\partial t}. \quad (76)$$

The nonlinear polarization vector  $\mathbf{P}^{(3)}(t)$  simplifies greatly, removing all anisotropic terms,

$$P_y^{\text{NL}}(t) = \varepsilon_0 [\chi_{\text{el}}^{(3)} E_y(t) [E_y(t)]^2 + E_y(t) S_a(t) + E_y(t) S_{b,yy}(t)], \quad (77)$$

$$P_y^{\text{NL}}(t) = \varepsilon_0 \chi_0^{(3)} E_y(t) \int_{-\infty}^{\infty} [f_{\text{el}} \delta(t-t') + f_a g_a(t-t') + f_b g_b(t-t')] E_y^2(t') dt', \quad (78)$$

which matches the simple example in [19], except this example is y-polarized instead of x-polarized.

The Newton-Raphson method simplifies to  $\mathbf{E}^{n+1} = \hat{\mathbf{a}}_y E_y^{n+1}$ ,

$$\begin{aligned} [Y] = & -\nabla \times \mathbf{H}^{n+1/2} + \frac{\varepsilon_0}{\Delta t} (\mathbf{E}^{n+1} \\ & - \mathbf{E}^n) + \frac{1}{2} \sum_{p=1}^3 \left[ (1 + \alpha_p) \mathbf{J}_{\text{Lorentz}_p}^n \right. \\ & \left. - \mathbf{J}_{\text{Lorentz}_p}^{n-1} + \frac{\gamma_p}{2\Delta t} (\mathbf{E}^{n+1} - \mathbf{E}^{n-1}) \right] + \chi_0^{(3)} f_{\text{el}} \frac{\varepsilon_0}{\Delta t} \{ (|\mathbf{E}^{n+1}|)^2 \mathbf{E}^{n+1} \\ & - (|\mathbf{E}^n|)^2 \mathbf{E}^n \} + \frac{\varepsilon_0}{\Delta t} (\mathbf{E}^{n+1} S_a^{n+1} - \mathbf{E}^n S_a^n) \\ & + \frac{\varepsilon_0}{\Delta t} (\mathbf{E}^{n+1} S_{b,yy}^{n+1} - \mathbf{E}^n S_{b,yy}^n), \end{aligned} \quad (79)$$

where,

$$[E_y^{n+1}]_{g+1} = [E_y^{n+1}]_g - (M_{\text{TE}}^{-1} [Y])|_g, \quad (80)$$

$$M_{\text{TE}} = \frac{1}{4\Delta t} \sum_{p=1}^3 \gamma_p + \frac{\varepsilon_0}{\Delta t} [1 + f_{\text{el}} \chi_0^{(3)} \{3(E_y^{n+1})^2\} + S_a^{n+1} + S_{b,yy}^{n+1}]. \quad (81)$$

Note how much simpler this version of the Newton-Raphson is than the prior two sections, since, due to only one electric field component there are no off diagonal terms.

## 3. Numerical Results and Analysis

In this section a 2D  $\text{TM}_z$  electromagnetic wave propagating in nonlinear isotropic material fused silica, is formulated and numerically simulated. The original FDTD GVADE 2D  $\text{TM}_z$  example from [1, 2] is reproduced using the nonlinear response tensor from [29] for fused silica

and the linear response and simulation parameters from [1, 2]. The goal of this simulation was to show a simple example and proof-of-concept, simulating an electromagnetic wave propagating in a nonlinear isotropic material with both isotropic and anisotropic parts of the polarization vector, illustrating how the extended FDTD GVADE method is implemented.

All the computational simulation results in this article were conducted with the advanced computing resources provided by Texas A&M High Performance Research Computing.

### 3.1 Simulation Results: Material and Parameters

The normalized nonlinear rank 4 material response tensor for silica written in a slightly modified form from [29] is,

$$\mathbf{g}_{ijkl}^{(3)}(t) = \left[ \frac{f_{el}}{3} \delta(t) (\delta_{ij}\delta_{kl} + \delta_{ik}\delta_{jl} + \delta_{il}\delta_{jk}) + f_a \mathbf{g}_a(t) \delta_{ij}\delta_{kl} + \frac{1}{2} [f_b \mathbf{g}_b(t) + f_c \mathbf{g}_a(t)] (\delta_{ik}\delta_{jl} + \delta_{il}\delta_{jk}) \right]. \quad (82)$$

The material parameters and the simulation parameters are listed in Table 1 and Table 2. In Table 1 for clarity, the variables  $f_{el}$ ,  $f_a$ ,  $f_b$  and  $f_c$  are written as products along with their actual value, to avoid any confusion since [29] defines  $f_a$ ,  $f_b$  and  $f_c$  differently than this paper, but the response tensor is equivalent, where  $f_m = f_R f_{m, [Lin and Agrawal 2006]}$  with  $m = a, b, c$ .

**Table 1. Material Parameters**

Parameter	Value
$\beta_1$	0.69617
$\beta_2$	0.40794
$\beta_3$	0.89748
$\omega_1$	$2.7537 \times 10^{16}$ rad/s
$\omega_2$	$1.6205 \times 10^{16}$ rad/s
$\omega_3$	$1.9034 \times 10^{14}$ rad/s
$n_2$	2.6e-20 m <sup>2</sup> /W
$\tau_1$	12.2 fs
$\tau_2$	32 fs
$\tau_b$	96 fs
$f_{el}$	(1-0.245)=0.755
$f_a$	(0.245)(0.75)=0.18375
$f_b$	(0.245)(0.21)=0.05145
$f_c$	(0.245)(0.04)=0.0098
$f_R$	0.245
$f_{R,Isotropic}$	0.18

From [1, 2, 19, 29, 31]

**Table 2. Simulation Parameters**

Parameter	Value
$\Delta z = \Delta x$	$5.333333 \times 10^{-9}$ meters
$\Delta t$	$3.34 \times 10^{-18}$ seconds
$nz$	22501
$n_x$	5001
$n$	25,000 time-steps
$\omega_c$	$4.35 \times 10^{15}$ rad/s ( $\lambda_0 \sim 433$ nm)
$w_0$	667 nm
$A_0$	$4.77 \times 10^7$ A/m

Some Values Selected From [1, 2, 32]

where  $\epsilon_r(\omega_c) = [n_0(\omega_c)]^2 = 2.15188$  and  $\chi_0^{(3)} = (4/3)c \epsilon_0 \epsilon_r n_2 = 1.98 \times 10^{-22}$  m<sup>2</sup>/W.

For comparison, the isotropic polarization vector response function is

$$\mathbf{g}_{ijkl}^{(3)}(t) = \left[ (1 - f_{R,Isotropic}) \delta(t) (\delta_{ij}\delta_{kl} + \delta_{ik}\delta_{jl} + \delta_{il}\delta_{jk}) + f_{R,Isotropic} \mathbf{g}_a(t) \delta_{ij}\delta_{kl} \right], \quad (83)$$

where  $f_{R,Isotropic}$  is slightly different than  $f_R$  as described by [19, 29]. This equation can be written more simply since the terms leading to the anisotropic polarization vector are removed,

$$\mathbf{P}_{Isotropic}^{NL} = \epsilon_0 \chi_0^{(3)} \mathbf{E}(\mathbf{r}, t) \int_{-\infty}^{\infty} \left[ g_{Isotropic}^{(3)}(t-t') |\mathbf{E}(\mathbf{r}, t')|^2 \right] dt', \quad (84)$$

$$g_{Isotropic}^{(3)}(t) = (1 - f_{R,Isotropic}) \delta(t) + f_{R,Isotropic} g_a(t). \quad (85)$$

The 2D  $TM_z$  fields were simulated using a  $n_x \times n_z$  dimension Lebedev grid [16, 33, 34], in the same manner as [32], except in this paper the simulation space was not cut in half using symmetry. Liu's paper [34] calls this grid the “unstaggered grid”, which is a combination of two shifted Yee grids with resulting in collocated electric field components. The two Yee grids are coupled through the nonlinear polarization current terms.

### 3.2 Simulation Results and Discussion

The hard source used to excite the electromagnetic wave at  $z = 0$  is [2]

$$H_y(t) = A_0 \sin(\omega_c t) \operatorname{sech}(x/w_0). \quad (86)$$

Simulation results of  $|\mathbf{E}|$  for the 2D  $TM_z$  case using both the original FDTD GVADE isotropic polarization vector model and the extended FDTD GVADE method are shown in Fig. 1.

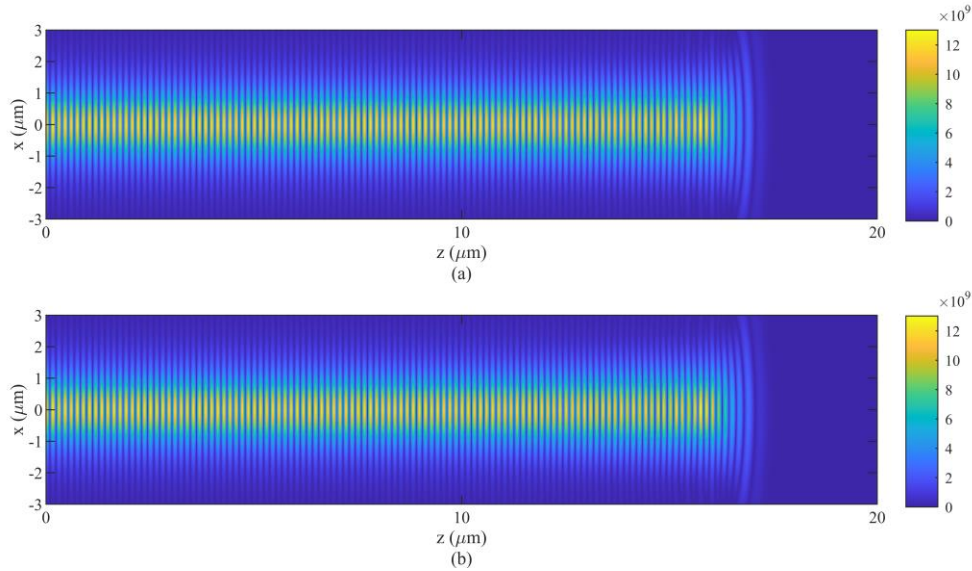


Fig. 1. Results of  $|\mathbf{E}|$  for 2D  $TM_z$  simulation with input amplitude  $A_0$ . (a) Original FDTD GVADE - Isotropic Polarization Vector, (b) Extended FDTD GVADE – Including Anisotropic Polarization Vector.

The half-power beamwidth (HPBW) and magnitude of the magnetic field,  $|H_y(z)|$ , at extremum locations curves are plotted versus propagation distance in Fig. 2. Also, simulation results for input amplitudes of  $1.02A_0$  and  $1.05A_0$  are shown in Fig. 2 as well, for the polarization vector including an anisotropic part, for comparison purposes. A “moving-mean” was used to smooth the curves allowing the behavior to be more easily seen and compared, while maintaining the shape of the curves.

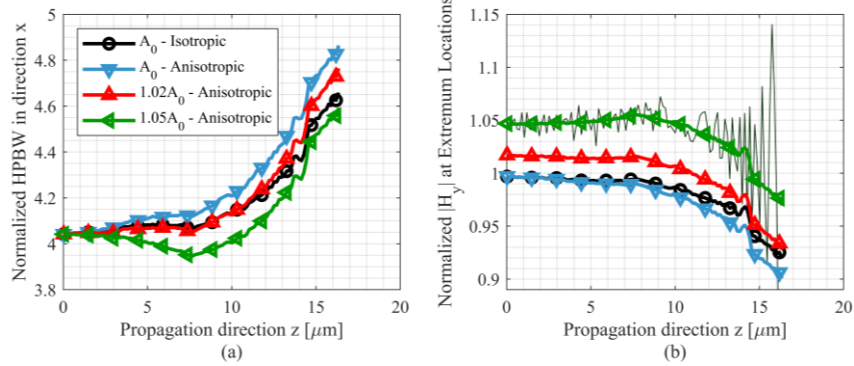


Fig. 2. Smoothed half-power beamwidth and magnetic field amplitude versus propagation distance  $z$  at the  $\sin(\omega_c t)$  extremum locations in the propagation direction  $z$ . (a) Smoothed HPBW( $z$ ) calculated relative to  $\max(|H_y(z)|)$  at each  $z$  location, normalized to the approximate material wavelength  $\lambda_d = \lambda_0/\sqrt{\epsilon_r}$ . (b) Smoothed  $|H_y(z)|$  at the extremum location, normalized to the  $|H_y(z = z_{nearest})|$ , where  $z_{nearest}$  is the nearest extremum location to  $z = 0$ . Note: For (b), the thinner darker green curve is the “unsmoothed”  $1.05A_0$  input amplitude case, illustrating the “moving-mean” smoothing process used for each curve in the figure.

By observation of the simulation results shown in Fig. 2., the extended version with the polarization vector including the anisotropic part appears to require a slightly larger input amplitude to produce the same HPBW as the wave propagates. Otherwise, the simulation results seem to be similar for fused silica. While this is a simple example, it does show that the isotropic polarization vector and more accurate model including the anisotropic part results vary slightly, and it seems reasonable to assume this variance could potentially be larger for material with larger anisotropic polarization vector components.

#### 4. Conclusion

In this paper we have presented an extension to the FDTD GVADE method, allowing the simulation of electromagnetic wave propagation at optical frequencies in nonlinear isotropic material with polarization vectors which include anisotropic components along with the isotropic component previously included. While more computationally expensive, this method allows for more accurate simulation of nonlinear optical material which has an anisotropic polarization vector component. A  $TM_z$  example using this method to simulate electromagnetic wave propagation in fused silica was performed, showing the usage of the extended FDTD GVADE method.

**Acknowledgments.** Caleb Grimms thanks Junseob Kim for his contribution by creating the initial 2D isotropic polarization vector FDTD GVADE code for his master’s thesis based on [1-3].

**Disclosures.** The authors declare no conflicts of interest.

**Data availability.** To the best of the authors’ knowledge, the data underlying the results presented in this paper are included in this paper but may also be obtained from the authors upon reasonable request.

**Honoring.** Part of the authors’ goal in writing this paper was to honor the late Dr. Allen Taflove and his contribution to the field of computational electromagnetics and the finite-difference time-domain method.

#### References

1. J. H. Greene, "Finite-difference time-domain model of resonator coupling and nonstationary nonparaxial spatial optical soliton focusing and scattering," in *Field of Electrical Engineering and Computer Science*(NORTHWESTERN UNIVERSITY, 2007), p. 95.

2. J. H. Greene, and A. Taflove, "General vector auxiliary differential equation finite-difference time-domain method for nonlinear optics," *Opt Express* **14**, 8305-8310 (2006).
3. Z. Lubin, J. H. Greene, and A. Taflove, "GVADE FDTD Modeling of Spatial Solitons," in *Artech Hse Antenn Pr*(2013), pp. 497-517.
4. P. D. Maker, and R. W. Terhune, "Study of Optical Effects Due to an Induced Polarization Third Order in Electric Field Strength," *Phys Rev* **137**, A801 (1965).
5. P. D. Maker, R. W. Terhune, and C. M. Savage, "Intensity-Dependent Changes in Refractive Index of Liquids," *Phys Rev Lett* **12**, 507 (1964).
6. C. C. Wang, "Nonlinear Susceptibility Constants and Self-Focusing of Optical Beams in Liquids," *Phys Rev* **152**, 149-& (1966).
7. D. H. Close, C. R. Giuliano, R. W. Hellwarth, L. D. Hess, F. J. McClung, and W. G. Wagner, "Self-Focusing of Light of Different Polarizations," *Ieee J Quantum Elect* **Qe 2**, 553 (1966).
8. E. Garmire, R. Y. Chiao, and C. H. Townes, "Dynamics and Characteristics of Self-Trapping of Intense Light Beams," *Phys Rev Lett* **16**, 347 (1966).
9. R. Hellwarth, J. Cherlow, and T. T. Yang, "Origin and Frequency-Dependence of Nonlinear Optical Susceptibilities of Glasses," *Phys Rev B* **11**, 964-967 (1975).
10. R. W. Hellwarth, A. Owyong, and N. George, "Origin of the Nonlinear Refractive Index of Liquid CCL4," *Physical Review A* **4**, 2342-2347 (1971).
11. A. Owyong, R. W. Hellwarth, and N. George, "Intensity-Induced Changes in Optical Polarizations in Glasses," *Phys Rev B-Solid St* **5**, 628-+ (1972).
12. R. W. Hellwarth, "3rd-Order Optical Susceptibilities of Liquids and Solids," *Prog Quant Electron* **5**, 1-68 (1977).
13. R. Y. Chiao, E. Garmire, and C. H. Townes, "Self-Trapping of Optical Beams," *Phys Rev Lett* **13**, 479-& (1964).
14. T. K. Gustafson, P. L. Kelley, R. Y. Chiao, and R. G. Brewer, "Self-Trapping in Media with Saturation of Nonlinear Index," *Appl Phys Lett* **12**, 165 (1968).
15. P. L. Kelley, "Self-Focusing of Optical Beams," *Phys Rev Lett* **15**, 1005 (1965).
16. A. Taflove, and S. C. Hagness, *Computational electrodynamics : the finite-difference time-domain method* (Artech House, 2005).
17. K. S. Yee, "Numerical Solution of Initial Boundary Value Problems Involving Maxwells Equations in Isotropic Media," *Ieee T Antenn Propag* **Ap14**, 302 (1966).
18. Y. S. Kivshar, and G. P. Agrawal, *Optical solitons : from fibers to photonic crystals* (Academic Press, 2003).
19. G. P. Agrawal, *Nonlinear fiber optics* (Academic Press, 2019).
20. S. Nakamura, Y. Koyamada, N. Yoshida, N. Karasawa, H. Sone, M. Ohtani, Y. Mizuta, R. Morita, H. Shigekawa, and M. Yamashita, "Finite-difference time-domain calculation with all parameters of Sellmeier's fitting equation for 12-fs laser pulse propagation in a silica fiber," *Ieee Photonic Tech L* **14**, 480-482 (2002).
21. S. Nakamura, N. Takasawa, and Y. Koyamada, "Comparison between finite-difference time-domain calculation with all parameters of Sellmeier's fitting equation and experimental results for slightly chirped 12-fs laser pulse propagation in a silica fiber," *Journal of Lightwave Technology* **23**, 855-863 (2005).
22. D. McMorro, N. Thantu, V. Kleiman, J. S. Melinger, and W. T. Lotshaw, "Analysis of intermolecular coordinate contributions to third-order ultrafast spectroscopy of liquids in the harmonic oscillator limit," *J Phys Chem A* **105**, 7960-7972 (2001).
23. K. J. Blow, and D. Wood, "Theoretical Description of Transient Stimulated Raman-Scattering in Optical Fibers," *Ieee J Quantum Elect* **25**, 2665-2673 (1989).
24. D. McMorro, N. Thantu, J. S. Melinger, S. K. Kim, and W. T. Lotshaw, "Probing the microscopic molecular environment in liquids: Intermolecular dynamics of CS2 in alkane solvents," *J Phys Chem-Us* **100**, 10389-10399 (1996).
25. P. M. Morse, and H. Feshbach, *Methods of theoretical physics* (McGraw-Hill, 1953).
26. R. P. Feynman, R. B. Leighton, and M. L. Sands, *The Feynman lectures on physics* (Basic Books, 2011).
27. R. W. Boyd, *Nonlinear optics* (Academic Press is an imprint of Elsevier, 2019).
28. G. P. Agrawal, *Nonlinear fiber optics* (Elsevier / Academic Press, 2007).
29. Q. Lin, and G. P. Agrawal, "Raman response function for silica fibers," *Opt Lett* **31**, 3086-3088 (2006).
30. D. Kincaid, and E. W. Cheney, *Numerical analysis : mathematics of scientific computing* (Brooks/Cole, 2002).
31. R. H. Stolen, J. P. Gordon, W. J. Tomlinson, and H. A. Haus, "Raman Response Function of Silica-Core Fibers," *J Opt Soc Am B* **6**, 1159-1166 (1989).
32. C. J. Grimms, and R. D. Nevels, "Rotationally symmetric transverse magnetic vector wave propagation for nonlinear optics," *Opt. Express*, submitted for publication (2024).
33. M. Nauta, M. Okoniewski, and M. Potter, "FDTD Method on a Lebedev Grid for Anisotropic Materials," *Ieee T Antenn Propag* **61**, 3161-3171 (2013).
34. Y. Liu, "Fourier analysis of numerical algorithms for the Maxwell equations," *J Comput Phys* **124**, 396-416 (1996).